VI. Guidance and Control Research

GUIDANCE AND CONTROL DIVISION

A. Effective Work Function of Metal Contacts to Vacuum-Cleaved Photoconducting CdS,

R. J. Stirn

1. Introduction

In a previous article (SPS 37-51, Vol. III, pp. 78–82), photoconductive gains greater than unity have been reported for CdS, even when one of the metal contacts on the sample has a work function ϕ_m greater than the electron affinity E_A of CdS, i.e., when the contact should have blocking characteristics. Similar results have now been found at JPL for metals deposited on crystals of photoconducting CdS that have been cleaved in a vacuum, thus eliminating possible interfacial effects. Such results imply that some mechanism is operating that allows transport of electrons through the contact in quantities, *above* those expected for thermionic emission over the barrier, at least for barrier heights for these same metals measured on more conducting CdS (Refs. 1 and 2). Thus, the barriers appear to be *lower* on photoconducting CdS than those measured in Ref. 2. However, electron transport *through* the barrier by tunneling via trap levels within the forbidden gap has not been completely ruled out.

The electron concentration at the boundary of the metal contact to vacuum-cleaved surfaces of photoconducting CdS is also being determined at various temperatures and light intensities by an analysis of stationary high-field domains in the range of negative differential conductivity. The preliminary data yield barrier heights that are lower than those published in Refs. 1 and 2, and are relatively insensitive to the metal; in addition, their values are strongly dependent on temperature and moderately dependent on light intensity. None of these phenomena is observed in nonphotoconducting CdS.

In the following, some preliminary data obtained at JPL from the high-field domain analysis are presented, as well as current published values of barrier heights for CdS with various metal contacts obtained by other techniques.

2. Effective Barrier Heights in Photoconducting CdS

In CdS crystals with an N-shaped negative differential conductivity range (due to field-enhanced freeing of holes from traps and, hence, enhanced recombination), stationary high-field domains attached to the cathode are

observed above a critical applied voltage (Ref. 3). Above that voltage, the current saturates and the steplike domains increase in width linearly with voltage, eventually filling up the entire crystal. Such domains can be conveniently observed by the Franz–Keldysh effect using band-gap light, because of the increased optical absorption in the region of higher field. Details of the theory and experimental setup will be presented in a future SPS article.

A boundary-value carrier concentration n_{II} can be determined uniquely from the values of the saturation current, the mobility, and the electric field within the domain. The latter value is obtained from the domain width–voltage relationship and crystal length. This boundary value n_{II} can be shown to be nearly equal to the carrier concentration at the interface n_c. Given this value of n_c, which is found to vary with temperature and light intensity, an effective barrier height can be derived from the expression

$$n_c = N_c \exp\left[-\phi_B/(kT)\right] \qquad (1)$$

where

$$N_c = 2\,(2\,\pi\,m^*kT/h^2)^{3/2}$$

$$= 2.3 \times 10^{18}\,(T/300)^{3/2}$$

is the effective density of states for CdS. The barrier height at the surface is denoted by ϕ_B. Actually, Eq. (1) is strictly valid only for thermodynamic equilibrium. Thus, in a photoconductor where generation of electrons and holes is taking place, this relationship (Eq. 1), is not exact. However, it is phenomenologically meaningful in that it helps in comparing different metal contacts.

The values of n_{II} (assumed to be equal to n_c) obtained from the analysis on vacuum-cleaved crystals of CdS for a photon flux density of $5 \times 10^{15}/\text{cm}^2/\text{s}$ ranged from 10^8 to $10^{10}/\text{cm}^3$. (The method of analysis will be discussed in a future SPS article.) The values of the saturation current density are typically 10^{-2} to 10^{-3} A/cm^2 and the electric field within the domain varies between 3.0×10^4 and 1.20×10^5 V/cm, depending on the metal and the light intensity. The electron mobility was assumed to be constant up to 4.0×10^4 V/cm and then drop as the inverse of the electric field above that value.[1]

[1]Böer, K. W., and Bogus, K., "Electron Mobility of CdS at High Electric Fields," to be published in *Phys. Rev.*

Calculated values of the effective barrier height are shown in Table 1 for the above photon flux density. The domains are very hard to see at the higher temperatures because of the decreased Franz–Keldysh effect. It can be seen that there is little difference between the metals, unlike those reported in Ref. 2 (Table 2). Also, there is a marked temperature dependence.

The light intensity dependence of ϕ_B for several samples is shown in Table 3. The light used was monochromatic and ranged from 512 to 490 nm, depending on the temperature (band gap). The range of intensity (flux

Table 1. Temperature dependence of the effective barrier height measured on photoconducting CdS

Temperature, °K	Effective barrier height, eV					
	Gold	Platinum	Silver	Nickel	Copper	Tin
155	0.30	0.27	—	—	0.27	0.26
180	0.35	0.30	0.34	0.31	0.32	0.29
220	0.42	0.36	—	0.37	—	0.35
255	0.47	—	0.47	—	0.44	—
295	0.53	0.50	0.53	—	—	—

Table 2. Summary of barrier heights on CdS (taken from Ref. 2)

Metal	Barrier height from photoresponse, eV	Barrier height from capacitance data, eV	Metal work function, eV
Platinum	0.85 ± 0.03	0.86 ± 0.02	5.0
Gold	0.78 ± 0.03	0.80 ± 0.05	4.7 (5.2)
Silver	0.56 ± 0.02	0.58 ± 0.03	4.4
Nickel	0.45	—	4.7
Copper	0.36	0.35 ± 0.03	4.5
Aluminum	Ohmic contact	—	4.2

Table 3. Light dependence of the effective barrier height measured on photoconducting CdS

Relative light intensity, %	Effective barrier height, eV		
	Gold (155° K)	Nickel (180° K)	Silver (295° K)
100.0	0.28	0.29	0.48
40.0	0.29	0.30	0.51
20.0	0.30	0.31	0.53
10.0	0.30	0.31	0.54
4.0	0.31	0.32	0.55
2.0	0.32	0.33	0.57
1.0	0.33	0.34	—

density) was varied by 100 with the highest value[2] $I_0 = 5 \times 10^{16}/cm^2/s$.

One can see that the effective barrier heights increase with decreasing light intensity. An interesting point is that at room temperature the values of ϕ_B (which are about the same for all six metals) tend to a zero light-intensity value, which is about equal to the energy of the bulk Fermi level ϕ_n (in the dark) as measured from the conduction-band edge. The Fermi level in the bulk of the crystal is obtained from the dark resistivity ρ_0 and the expressions

$$\left. \begin{aligned} n &= N_c \exp\left[-\phi_n/(kT)\right] \\ \rho_0 &= (q\,n\,\mu)^{-1} \end{aligned} \right\} \qquad (2)$$

where n is the bulk free-carrier concentration and q is the electronic charge. The mobility μ can be assumed to follow a T^{-2} law quite accurately between 100 and 300°K (Ref. 4), and to have a value of 300 cm²/V-s at 300°K. Then,

$$\phi_n = kT \ln\left[N_c\,(q\,\mu\,\rho_0)\right]$$

$$= kT \ln\left[2.5 \times 10^{18} \left(\frac{T}{300}\right)^{3/2} q \cdot 300 \left(\frac{T}{300}\right)^{-2} \rho_0\right]$$

$$= kT \left[4.75 + \tfrac{1}{2}\ln\left(\frac{300}{T}\right) + \ln\rho_0\right] \qquad (3)$$

A room temperature value of about 0.60 eV was obtained for the crystals used in this report, and a value of 0.34 eV at 155°K.

It would be very desirable to measure the barrier heights by the technique of high-field domains on crystals having different resistivities, i.e., Fermi-level positions, and look for any possible correlation. However, it has not been possible up to this time to dope the CdS crystals in order to get substantially different resistivities and still obtain the required stationary domains.[3]

3. Photoconductive Gains

As noted in the *Introduction,* gains greater than unity are observed in these crystals even though the published barrier heights for the metal–CdS (see *Subsection 4*) are

[2]This value of photon flux density drops slightly to $4 \times 10^{16}/cm^2/s$ at the lowest temperatures because of the shift in band gap (wavelength) with temperature and the nonlinear monochromator output.

[3]The crystals used in this investigation, purchased from the University of Delaware, are slightly doped with silver and aluminum.

of such magnitude that the contact should be completely blocking. The concept of gain in a photoconductor was reviewed in the previous article (SPS 37-51, Vol. III). The gain factor, expressed as the ratio of the saturation current to the photon flux density absorbed times the charge of an electron, has been measured to be at least 4 or 5 in these samples. The actual gain at the contact (in the domain) is at least 10 times higher because a stable domain can be formed with less than a tenth of the sample length ($\sim$ 0.5 to 1.0 mm). It is this length (volume) which should be considered in the light absorption since it is the domain region that is controlling the gain factor. The contribution of the rest of the crystal only reduces the gain factor because of the presence of recombination. In fact, the measured gains are lower than what might be because of considerable thermal quenching in these samples.[4] For this reason, no formal table of gain factors versus metal contact or temperature, for example, is given. The bulk characteristics and sample geometry considerably limit the gain possible with these contacts.

4. Published Values of Barrier Heights on Semiconducting CdS

A review of the three types of measurements used for barrier-height studies (photoresponse, diode forward characteristic, and differential capacitance) was given in SPS 37-51, Vol. III, as well as a description of barrier parameters. A large number of vacuum-cleaved semiconductors with various metal contacts were investigated by Spitzer and Mead (Refs. 1 and 2). Of a total of 14 different semiconductor materials of the diamond group IV or zincblende III–V types, with band gap covering a factor of 40 in energy, all but 3 (InAs, InP, and GaSb) exhibit a barrier height nearly equal to one-third of the band gap as measured from the valence-band edge. This value was nearly independent of the metal work function, which indicates that surface states play a major role in these materials in determining the barrier height. Another exception (in the wurzite II–VI class) was CdS, where the barrier height did depend in some way on the metal work function. The barrier heights found in their samples of CdS, which had carrier densities ranging from 10^{15} to 10^{17}, are listed in Table 2. Data from both photoresponse and capacitance–voltage measurements are given. The second figure in each column ($\pm$) gives the variation found from sample to sample. Substantial difference can be seen between the values in Tables 2 and 3.

[4]Thermal quenching in a photoconductor is the reduction of photocurrent because of increased recombination due to thermal releasing of holes from traps. A similar effect is seen for infrared quenching.

Many other investigators have published data on barrier heights of metal contacts evaporated or plated onto CdS thin films or crystals, which have been exposed to air or etched. The values are higher for some metals and lower for others. These values and results obtained at JPL on air-cleaved crystals of CdS, using the analysis presented in Subsections 2 and 3, will be discussed in a future SPS article.

The particular values of ϕ_B obtained for lower resistivity CdS from photoresponse measurements, for example, are not seriously in question here. However, the preliminary results of this work show that the interpretation of barrier heights on photoconductors, if indeed one can define a barrier height in this nonequilibrium situation, needs to be thoroughly investigated. In fact, much more work is needed in the case of the relatively few semiconducting materials that show differences in contact properties from metal to metal. The simple relationship

$$\phi_B = \phi_m - E_A \qquad (4)$$

which is then used in these cases, can give misleading results. This is due to the fact that ϕ_B is the difference between two numbers nearly equal in magnitude. The value of the metal work function ϕ_m, in turn, is an average of many determinations made by different experimenters whose results have been strongly influenced by the surface purity of the metal. In addition, metal thin films probably have a different work function than bulk crystals. Most serious is the apparent fact that the value of ϕ_m for thin films depends strongly on the substrate which is used. This effect has been demonstrated for gold in an elegant experiment (Ref. 5), where the values of ϕ_m varied from 5.08 to 5.40 to 5.59 eV, when the substrate was changed from CdTe to polished stainless steel to CdS, respectively. In addition, these values are well above the commonly used values of 4.7 eV. Good agreement with the higher values has been reported recently (5.2 eV) by two other investigators (Refs. 6 and 7), who demonstrated that mercury contamination was the cause of the lower value of 4.7 eV. Thus, the values of ϕ_B in Table 2 are not in order of ϕ_m, especially if the higher value of 5.6 eV for ϕ_m is used for gold on CdS. (Also note the position of nickel.)

It should be pointed out that Swank (Ref. 5) did obtain a barrier height of 0.80 eV for gold on semiconducting CdS in agreement with Ref. 2. This required a revision of the value of the electron affinity for CdS. The new value reported by Swank is 4.8 eV, as compared to the previously accepted value of 3.9–4.0 eV.

5. Conclusions

The results of Subsections 2 and 3, if the analysis using high-field domains is correct, show that the concepts of contact barriers on photoconductors are not useful when relatively high currents are flowing. For the latter situation, it appears that the barrier height between the metal and CdS is effectively lowered, allowing much larger gain factors than would normally be expected.

Additional investigations on different metals contacted to CdS, with varied amounts of doping, would be desirable. Extension of the measurements to light intensities far lower than those required to actually see the domain is also needed in order to observe the effect of decreasing current densities.

References

1. Spitzer, W. G., and Mead, C. A., "Barrier Height Studies on Metal-Semiconductor Systems," J. Appl. Phys., Vol. 34, p. 3061, 1963.

2. Mead, C. A., and Spitzer, W. G., "Fermi Level Position at Metal-Semiconductor Interfaces," Phys. Rev., Vol. 134, p. A713, 1964.

3. Böer, K. W., and Voss, P., "Stationary High-Field Domains in the Range of Negative Differential Conductivity in CdS Single Crystals," Phys. Rev,. Vol. 171, p. 899, 1968.

4. Physics and Chemistry of II-VI Compounds, p. 581. Edited by M. Aven and J. S. Prener. North-Holland Publishing Co., Amsterdam, 1967.

5. Swank, R. K., "Surface Properties of II-VI Compounds," Phys. Rev., Vol. 153, p. 844, 1967.

6. Huber, E. E., "The Effect of Mercury Contamination on the Work Function of Gold," Appl. Phys. Lett., Vol. 8, p. 169, 1966.

7. Riviere, J. C., "The Work Function of Gold," Appl. Phys. Lett., Vol. 8, p. 172, 1966.

B. Preliminary Results From Switching Experiments on MnBi Films, G. W. Lewicki and J. E. Guisinger

1. Introduction

The role of Curie-point switching in a proposed high-density magneto-optic memory utilizing MnBi films has been described in SPS 37-42, Vol. IV, pp. 59–61; theoretical aspects of this switching have been considered in SPS 37-46, Vol. IV, pp. 84–87. This article describes the experimental apparatus used for normal and Curie-point-switching experiments, and discusses the significance of some preliminary results with respect to memory and recording applications.

2. Experimental Apparatus

A block diagram of the apparatus used in the switching experiments is given in Fig. 1. For visual observation of domain structure, an MnBi film is situated within an electromagnet with hollow pole pieces, illuminated with light from a xenon arc lamp passed through polarizer 1, and viewed through polarizer 2. Polarizer 2 can be set so that areas having opposite average magnetizations appear as light and dark regions. This can be done because the rotation of plane-polarized light passing through the film is proportional to the average magnetization within the film. The transmission by the film–polarizer 2 combination of plane-polarized light represents a measure of the average magnetization within the film. The electromagnet allows the generation of a magnetic field perpendicular to the plane of the film. The strength of this field is monitored by a Hall probe.

For the purpose of electronically measuring average magnetization, a small amount of laser radiation (0.1 mW) is allowed to pass through the Pockel's cell, polarizer 1,
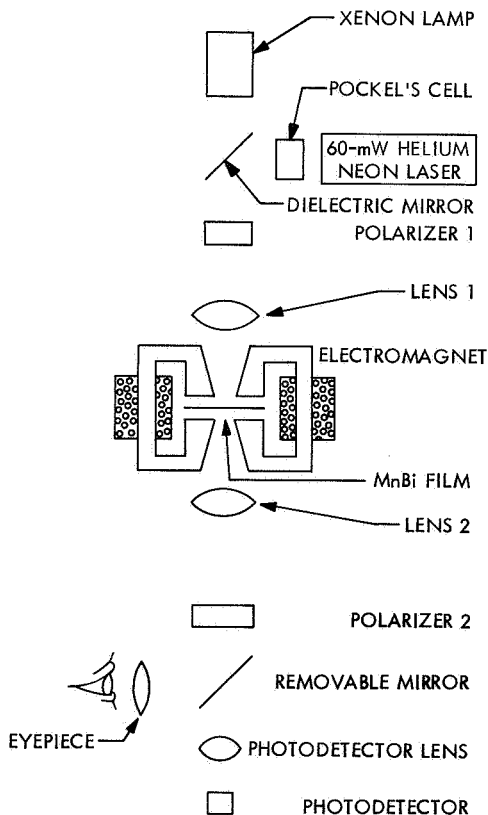
the film, and polarizer 2, and is collected by a photodetector. The output of the photodetector is used as a measure of the average magnetization within the film.

For Curie-point switching, a high-voltage pulse is fed into the Pockel's cell to allow some 15 mW of laser radiation to be focused onto a 2-μm spot on the film for approximately 1 μs. This amount of incident optical energy is sufficient to heat a 1-μm spot on the film past its Curie temperature. The spots, upon cooling, acquire an average magnetization dependent on the value of magnetic field applied during the switch.

3. Normal Switching Characteristics of 700-Å MnBi Films

Normal switching refers to changing the average magnetization within a film with an applied magnetic field without heating the film by the laser beam. Typical major and minor loop plots of the average magnetization as a function of applied field are shown in Fig. 2.

The average magnetization versus applied-field loop that is generated by a varying field, which does not reverse itself until the film becomes magnetically saturated, is called a major loop. A minor loop is generated by a varying field that reverses itself before the film is magnetically saturated.

For a major loop, a very high field ($H > 3.5\,\mathrm{kOe}$) is applied so that the film becomes magnetically saturated (the film is completely magnetized in the direction of the applied field with an average magnetization equal to the saturation magnetization). When the field is reduced to zero value, the film remains magnetically saturated. Only when the field is taken to a negative value coercive force ($-H_c$) does the average magnetization respond by suddenly dropping. This drop corresponds to the sudden appearance of domain structure or areas of opposite magnetization having the appearance of tree branches with doughnuts for leaves. This structure is shown in Fig. 3a; the size of the doughnuts is on the order of 5 to 10 μm. As the field is taken to still larger negative values, more and more of the tree-like structure appears suddenly (Fig. 3b) to give the film a negative average magnetization. As the field is taken to very large negative values, the film becomes magnetically saturated with its magnetization in the direction of the applied field. When the field is taken back to very high positive values, a similar process occurs.

The salient feature of the experimentally observed major loop is that 700-Å films have a large coercive force H_c ($H_c \approx 1\,\mathrm{kOe}$). Consequently, once a film is saturated,

Fig. 1. Block diagram of experimental apparatus used for switching experiments
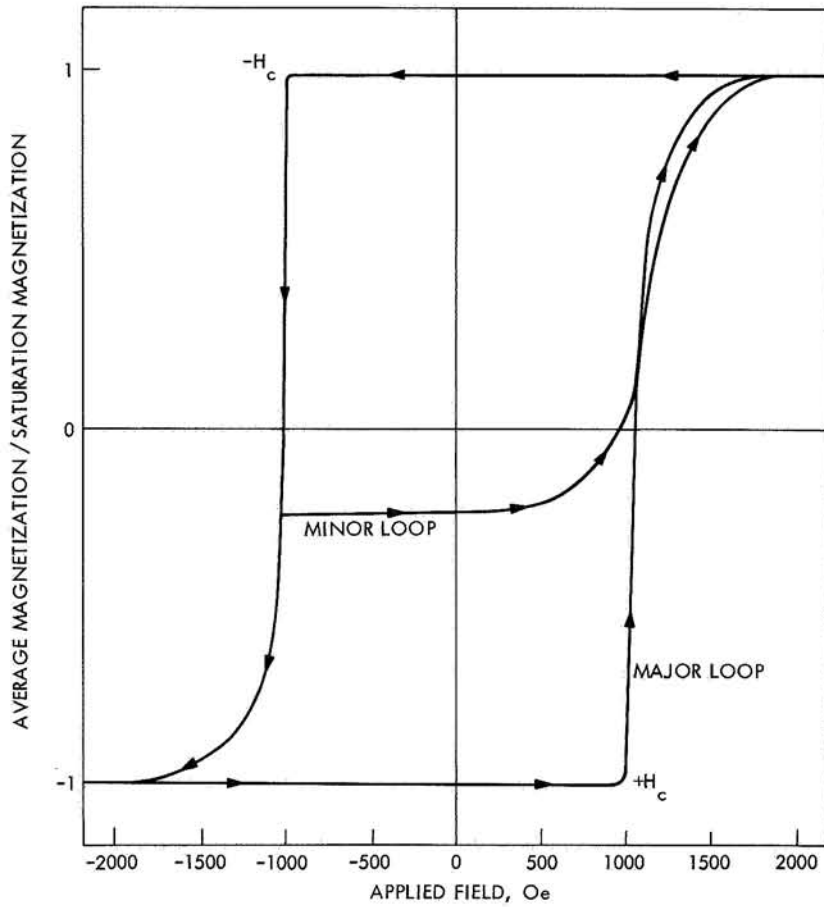
Fig. 2. Major and minor loops of the ratio of average magnetization
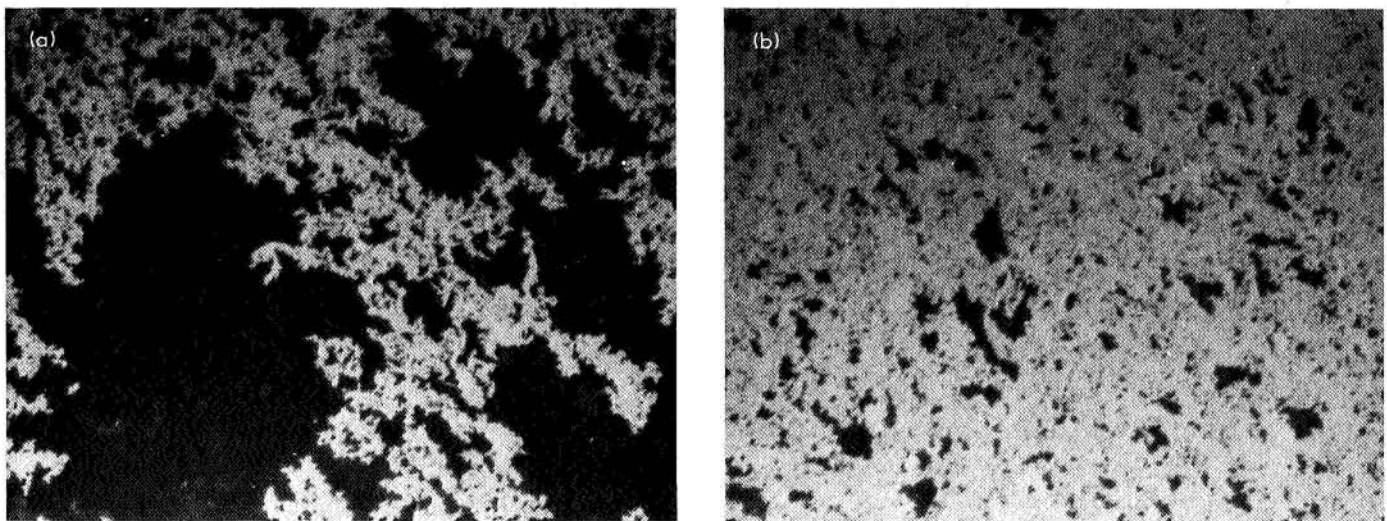to saturation magnetization as a function of applied field
for 700-A MnBi film

Fig. 3. Domain structure during normal switching of MnBi film: (a) partially switched, (b) further switched

large magnetic fields $H < H_c$ with directions opposite to that of the magnetization do not affect the film. During Curie-point switching of saturated films, fields opposed to the magnetization $H < H_c$ can be applied to influence the areas being Curie-point-switched without affecting other areas of the film. It has been observed that the coercive force decreases as the film thickness increases, becoming zero at a thickness of approximately 2500 Å. Lack of absolute reproducibility of coercive force from film to film has prevented the measurement of this dependence.

An interesting phenomenon was discovered upon visual observation of films being taken through minor loops such as the one shown in Fig. 2. Starting with the domain structure shown in Fig. 3a, when the field was varied in the direction to make the structure disappear, rather than make more of it appear (see the minor loop shown in Fig. 2), the structure did not suddenly disappear at a critical field as suddenly as it had appeared. Instead, it slowly turned from white to gray to black until the film was again magnetically saturated. Even with optics of high numerical aperture, the boundaries between light and dark regions could not be observed to move.

This observation indicates that the tree-like structures are not areas completely magnetized in one direction,

but blocks of oppositely magnetized domains smaller than the wavelength of light, the preponderance of fine domains magnetized in one direction over fine domains magnetized in the other direction determining the shade of gray of the block. Thus, a 1-μm discrete spot of 700-Å-thick MnBi film will probably not be a single domain, and, thus, will not be a magnetically bistable element for Curie-point switching, as discussed in SPS 37-46, Vol. IV.

4. Curie-Point Switching Characteristics of 700-Å MnBi Films

Small areas of a magnetically saturated MnBi film (surface dimension on the order of 1 μm) were Curie-point-switched with different values of magnetic field applied during the switch. The average value of the magnetization within the areas following the Curie-point switching was sensed with a photodetector. A plot of the resulting average magnetization as a function of the field applied during the switch is shown as a solid line in Fig. 4. The offset of the curve is explained by the fact that an area being Curie-point-switched is acted upon not only by the applied field but also by the demagnetizing field of the surrounding film (SPS 37-42, Vol. IV). The dotted line represents the normal switching characteristic of the film.
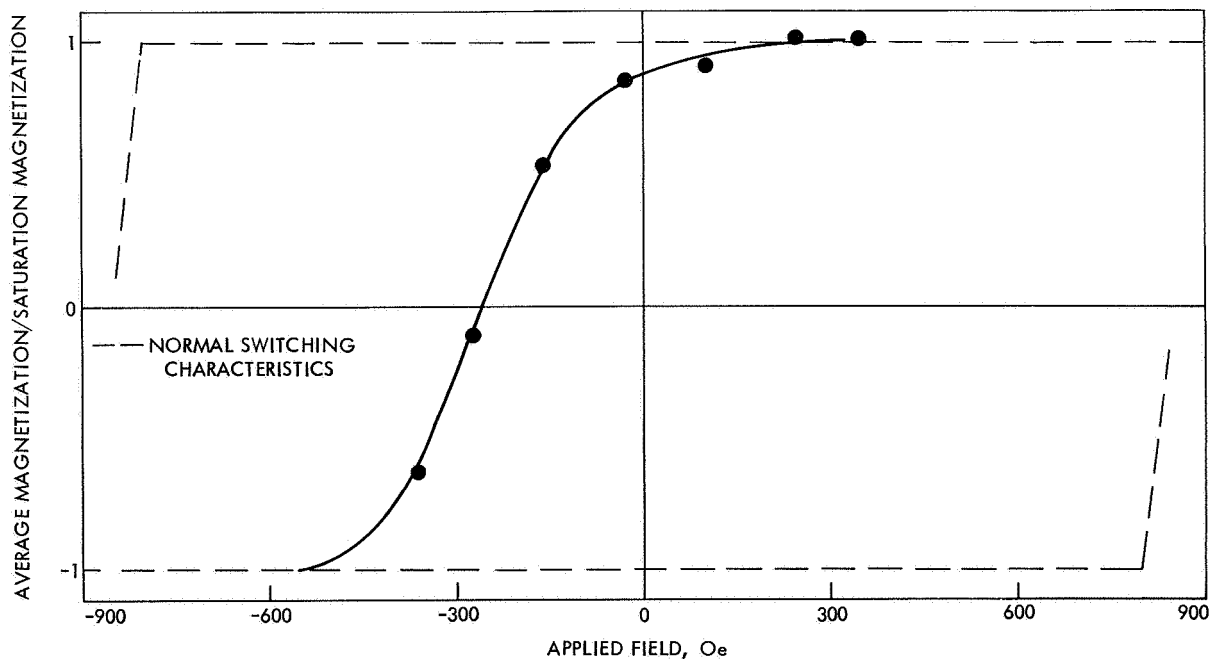

Fig. 4. Ratio of average magnetization to saturation magnetization of Curie-point-switched 1-μm spot on magnetically saturated MnBi film as a function of field applied during switching

The salient feature of this result is that the switching is not binary. Any value of average magnetization can be attained simply by varying the value of applied field during Curie-point switching. The result reaffirms the view that the basic domain size within a film 700 Å thick is much smaller than the wavelength of light.

Although not completely verified experimentally, it appears that there does exist a wide range of applied fields (-350 Oe $< H < -150$ Oe) in Fig. 4, which does not affect the average magnetization within an area that has been Curie-point-switched. This phenomenon is important for any recording application utilizing Curie-point switching in MnBi films.

5. Memory and Recording Applications

Application of MnBi films to the magneto-optic mass-memory scheme (SPS 37-42, Vol. IV) requires discrete areas of film that can be switched with reasonable values of applied field, i.e., no larger than tens of oersteds. The result shown in Fig. 4 implies that some 175 Oe above that required to compensate for demagnetizing fields would be required to switch such an area.

Theoretical considerations given in SPS 37-46, Vol. IV, suggest that a spot heated past its Curie temperature is completely switched by the smallest field when cooled to just below its Curie temperature. The relevant parameter in this situation is the ratio of field to saturation magnetization H/M_s; this ratio is very large at that temperature even for very small H since M approaches zero at the Curie temperature. However, upon further cooling, M_s increases and the completely switched spot can revert to multi-domain configuration, i.e., become unswitched, if both of the following conditions are satisfied: (1) the single-domain spot does not represent a lower energy state as compared to a multi-domain spot, and (2) there does not exist a sufficiently high energy barrier separating the single-domain spot configuration and the multi-domain spot configuration.

The data given in Fig. 4 show that a 1-μm discrete spot would favor a multi-domain configuration. However, they do not show the absence of a sufficiently high energy barrier separating the single-domain and the multi-domain states for a discrete 1-μm spot cooling from its Curie temperature because the data shown correspond to a continuous film.

Experiments are currently being performed to determine the Curie-point-switching fields for discrete areas. If discrete-area experiments yield a result similar to that

given in Fig. 4, another avenue of approach can be taken. Theory suggests that the basic domain size becomes large for very thin films, and also for thick films. One-μm domains have been observed in films having a thickness of 1 μm. A 1-μm discrete spot of this thickness film should favor a single-domain state, and thus be amenable to Curie-point switching with very small fields. Work in this direction is also being pursued.

The results obtained from Curie-point-switching experiments on continuous 700-Å MnBi films that seemingly have negative value for memory applications have positive value for recording applications. They suggest the following recording technique.

A high-intensity focused laser beam would be scanned across a magnetically saturated MnBi film to Curie-point-switch a track. The average magnetization along the track would be controlled by the magnetic field present during Curie-point switching of that portion of the track. This magnetic field would be limited to a range where it would not affect anything previously recorded on the track. By controlling the applied magnetic field during Curie-point switching, a time-varying signal could be recorded as a spatial variation of the average magnetization along the tracks of an MnBi film. The recording could then be read out by rescanning the track with a low-intensity laser beam and sensing the average magnetization along the track with a polarizer and photo-detector. A laser-beam scanning system is being assembled to further determine the physics relevant to such an application.

C. Fabrication of Small-Area $p^+\pi p^+$ Solid-State Diodes for Noise Measurements, A. Shumka

A program was established to investigate noise in germanium solid-state diodes.[5] Design criteria were established for optimizing these structures for noise measurements. The following guidelines were chosen:

(1) A $p^+\pi p^+$ structure to be used instead of the usual $n^+\pi n^+$ structure (SPS 37-39, Vol. IV, pp. 49–51) because it has an ohmic region in its I–V characteristic that can be effectively used for calibrating the noise analyzer.

(2) The input impedance of the solid-state diode to be of the order of 10 kΩ for operation within the maximum sensitivity range of the noise analyzer.

(3) The dc operation of the solid-state diode to extend well into the space-charge-limited (SCL) region before heating effects became important.

(4) Contacts to be alloyed because it was anticipated that they would not exhibit a large $1/f$ component of noise.

For these requirements to be satisfied, the solid-state diode was to have two p^+ contacts of 0.125-mm diameter alloyed on a π-type germanium wafer (acceptor doping density $\sim 10^{12}$ cm^{-3}). The separation between the contacts was to be 20 to 30 μm.

The contacts of 0.125-mm diameter specified for the $p^+\pi p^+$ solid-state diodes are much smaller than those of 0.5 and 0.7-mm diameter previously fabricated. The large reduction in contact area precluded the use of the masking and aligning techniques reported in SPS 37-32, Vol. IV, pp. 64–67. An optical system was constructed for defining and aligning the contacts through the use of photo-resist techniques.

Definition of the contact was obtained by placing a 0.125-mm circle, unexposed to light, on a thin layer of positive-working photo-resist, coated on a germanium wafer. This was accomplished by projecting onto the wafer a shadow from a 1.3-mm opaque disk that was placed in a beam of light from a mercury-arc lamp. A 7× microscope objective was used for focusing and reducing the image to required dimensions. The sensitized layer of photo-resist was dissolved in a developer. Positioning of the contact was performed with a special holding fixture that had a rotatable vacuum chuck for the wafer mounted on a three-axis micropositioner.

The photo-masking procedures were as follows: a thin and uniform layer of Shipley AZ1350 photo-resist was brushed on a wafer. Prior to mounting the wafer in the vacuum chuck, an optical filter (Schott-GG14) was inserted, which permitted the exposure of the specimen without sensitizing it. The wafer was rotated until it was aligned with the vertical and horizontal axes of the positioner and translated until an image of the disk was focused and centered. A beam splitter was used to monitor these operations with a microscope. After removal of the filter, an exposure time of about 4 s was sufficient to sensitize the photo-resist. The photo-resist mask took 2 min to develop. A SiO film was deposited on the masked surface. The photo-resist mask was subsequently dissolved in acetone, leaving the contact surrounded by the deposited SiO film. An identical procedure was then followed for the opposite side of the wafer. By this method the contact diameters could be controlled to within 5 μm and aligned to within 15 μm. The alloying techniques discussed in SPS 37-32, Vol. IV, could now be applied.

The germanium wafers were 2.5 mm square with a nominal thickness of 45 μm. To satisfy the requirement that the contacts be 20 to 30 μm apart, the penetration depths of the indium-alloyed contacts were controlled. Calculations based on the germanium–indium phase diagram were used to determine the amounts of indium necessary for alloying. There was a tendency for alloy pits to form because of the small contact areas, which made it difficult to control the penetration depths within 5 μm. Despite these alloy pits, which were larger in area than the contacts, it was found from metallurgical cross sections that the recrystallized p^+ contacts were defined by the mask only.

An I–V characteristic is shown in Fig. 5 for one of the $p^+\pi p^+$ solid-state diodes at dry-ice temperature. Three straight lines are drawn to depict the ohmic region and two SCL current regions, the uppermost region being related to the saturation of hole drift velocity. This solid-state diode can operate at a dc current as high as 8 mA, which is well within the SCL current region before any heating effects are observed. The I–V characteristics and the noise in the $p^+\pi p^+$ solid-state diode will be reported in a future SPS.
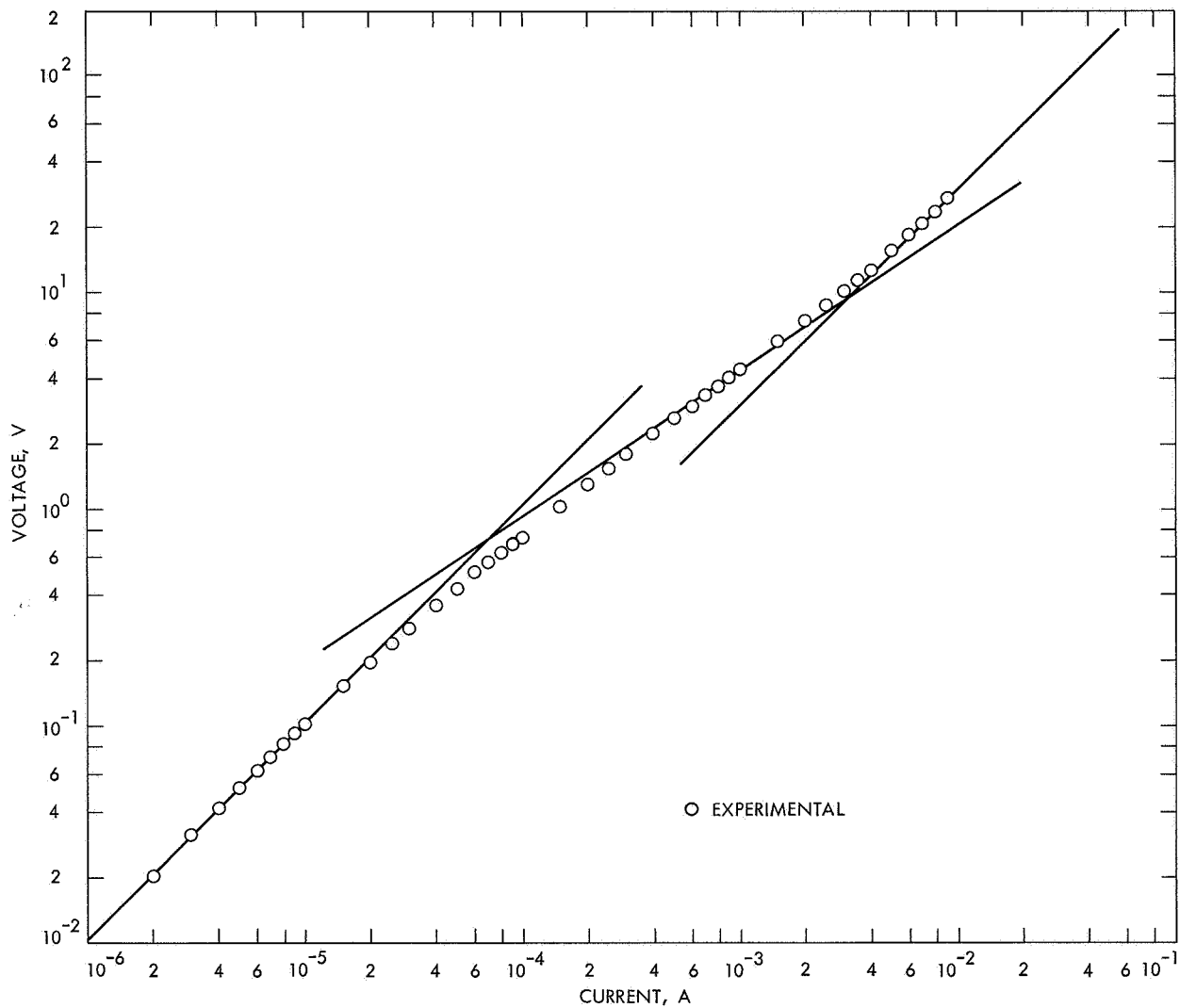
Fig. 5. _I–V_ characteristic of a _p⁺πp⁺_ solid-state diode at _T_ = 195°K